engineering proceedings

MDPI

Proceeding Paper

Solvothermal Synthesis of Nanomagnetite-Coated Biochar for Efficient Arsenic and Fluoride Adsorption †

Diego-Antonio Corona-Martinez [1], Lourdes Díaz-Jiménez [2], Audberto Reyes-Rosas [3], Alejandro Zermeño-González [4], Luis Samaniego-Moreno [4] and Sasirot Khamkure [5,*]

[1] Basic Science Department, Universidad Autónoma Agraria Antonio Narro, Saltillo 25315, Coahuila, Mexico; diegoa.coronam@uaaan.edu.mx
[2] Sustainability of Natural Resources and Energy, Centro de Investigación y de Estudios Avanzados del Instituto Politécnico Nacional, Saltillo 25900, Coahuila, Mexico; lourdes.diaz@cinvestav.edu.mx
[3] Department of Bioscience and Agrotechnology, Centro de Investigación en Química Aplicada, Saltillo 25294, Coahuila, Mexico; audberto.reyes@ciqa.edu.mx
[4] Irrigation and Drainage Department, Universidad Autónoma Agraria Antonio Narro, Saltillo 25315, Coahuila, Mexico; azermeno@uaaan.edu.mx (A.Z.-G.); luis.samaniego@uaaan.edu.mx (L.S.-M.)
[5] Irrigation and Drainage Department, SECIHTI-Universidad Autónoma Agraria Antonio Narro, Saltillo 25315, Coahuila, Mexico
* Correspondence: skhamkure@secihti.mx

† Presented at the 5th International Electronic Conference on Applied Sciences, 4–6 December 2024; https://sciforum.net/event/ASEC2024.

Abstract: Arsenic contamination in water demands effective, low-cost removal methods. This study introduces nanomagnetite-coated biochar derived from pecan nutshells for efficient arsenic adsorption. Utilizing a solvothermal method, uniform magnetite crystals were grown on biochar in a controlled process at 200 °C. The resulting bioadsorbent, characterized by XRD, SEM, and FTIR, exhibited a narrow size distribution and consistently high arsenic removal rates (97.30–98.76%). Biochar with varied particle sizes, synthesized at a short reaction time (6 h), showed the highest removal efficiency of arsenic (98.76%) and adsorption capacity (7.974 mg/g). This approach offers a sustainable for arsenic remediation, and ease of magnetic separation.

Keywords: arsenic contaminant; biochar; nanomagnetite; solvothermal

check for updates

Academic Editor: Ning Li

Published: 16 May 2025

Citation: Corona-Martinez, D.-A.; Díaz-Jiménez, L.; Reyes-Rosas, A.; Zermeño-González, A.; Samaniego-Moreno, L.; Khamkure, S. Solvothermal Synthesis of Nanomagnetite-Coated Biochar for Efficient Arsenic and Fluoride Adsorption. *Eng. Proc.* **2025**, *87*, 67. https://doi.org/10.3390/engproc2025087067

1. Introduction

While arsenic (As) and fluoride (F^-) are naturally occurring elements found in the environment and can be present in groundwater sources, their presence is a serious concern [1,2]. The International Agency for Research on Cancer has classified arsenic as a primary carcinogen due to its high toxicity. Exposure, even at low levels, can lead to arsenic poisoning and a range of adverse health effects Therefore, arsenic contamination of groundwater poses a significant health risk, so it is essential to find alternative and effective methods to eliminate it. There are various methods to remove arsenic from groundwater, like precipitation, ion exchange, solvent extraction, filtration, and adsorption [3]. However, these methods can be expensive, generate a high quantity of waste, or can be difficult to separate from the water. Nevertheless, the adsorption process can be a proven alternative to clean arsenic from groundwater, since it is efficient and relatively inexpensive and can be easily enhanced by reducing the particle size of the absorbent or modifying the surface [4].

Also, it is important to recognize that the literature shows great effort to produce magnetite nanoparticles because they present some interesting properties, such as high magnetization, low toxicity, and mainly because of the property of adsorption of heavy metals from water and wastewater [5–9]. However, the nanoparticles of magnetite are prone to aggregate, which can reduce the adsorption capacity [10]. Therefore, it is important to improve the particles by modifying the surface or, as in this research, creating a surface suitable for the direct growth of nanoparticles, achieving a homogeneous particle size and good dispersion, and improving the adsorption capacity of the nanomagnetite [11].

This research explores the alternative of nanomagnetite-coated biochar derived from pecan nut shells as an efficient arsenic adsorbent. By using solvothermal synthesis, magnetite nanoparticles are directly crystallized onto the surface of biochar particles. This method ensures a homogeneous coating with uniform size and requires short reaction times at low temperatures, eliminating the need for additional treatments [12]. The resulting particles exhibit enhanced arsenic and fluoride adsorption capacity.

2. Materials and Methods

Nanomagnetite-coated biochar was synthesized in a 45 mL autoclave. Pecan nutshells were ground, sieved (0.10–0.18 mm), and pyrolyzed (700 °C, 1 h, N_2) to produce biochar (0.18–0.38 mm). A solvothermal reaction, using ethylene glycol, trisodium citrate, urea, and iron(III) chloride, was performed. Iron chloride was dissolved in ethylene glycol, followed by the addition of trisodium citrate and urea. Biochar was then added at a 1:1 Fe^{3+} ratio. This reaction was conducted at 200 °C for 6–12 h, varying by sample group. The resulting particles were washed, magnetically separated, and dried 60 °C for 12 h.

The experimental design included three samples: S11 (control, magnetite only, 10 h reaction), S15 (biochar, 0.105–0.18 mm, 6 h reaction), and S16 (biochar, 0.18–0.38 mm, 6 h reaction). All samples were subjected to the solvothermal reaction. Three samples were tested for arsenic and fluoride adsorption. Arsenic adsorption was assessed at 3 mg/L initial concentration, pH 3, and a 2 g/L dose for 24 h. Fluoride adsorption was evaluated at 10 mg/L, pH 2, 2 g/L dose for 4 h. Arsenic was measured by an ICP-OES Analyzer (iCAP7400 Duo, Thermo Scientific, Waltham, MA, USA), and fluoride with an ion-selective electrode (9609BNW, Thermo Scientific, USA).

The synthesized nanomagnetite-coated biochar was characterized for structure, morphology, and surface functionality using XRD (PW3040, Xpert-Philips, Almelo, Netherlands), scanning electron microscopy (SEM) with EDS microanalysis system (XL 30 ESEM, Philips, Eindhoven, The Netherlands), Fourier Transform Infrared Spectroscopy (FTIR, Frontier IR/NIR, PerkinElmer, Waltham, MA, USA).

3. Results

3.1. Characterization of Nanomagnetite-Coated Biochar

The XRD patterns of samples S11, S15, and S16, displayed in Figure 1, exhibit characteristic peaks that align with the standard diffraction peaks for magnetite (Fe_3O_4) as indicated by the JCPDS reference 19-0629. The pattern for sample S11 shows well-defined and relatively high-intensity peaks at the positions corresponding to the standard magnetite peaks. These peaks include prominent reflections at the positions marked as (311), (440) and other less intense reflections such as (220), (111), (222), (400), (511), (422), (333), (620), (533), (622), and (444), indicating a relatively high degree of crystallinity and a well-formed magnetite structure.

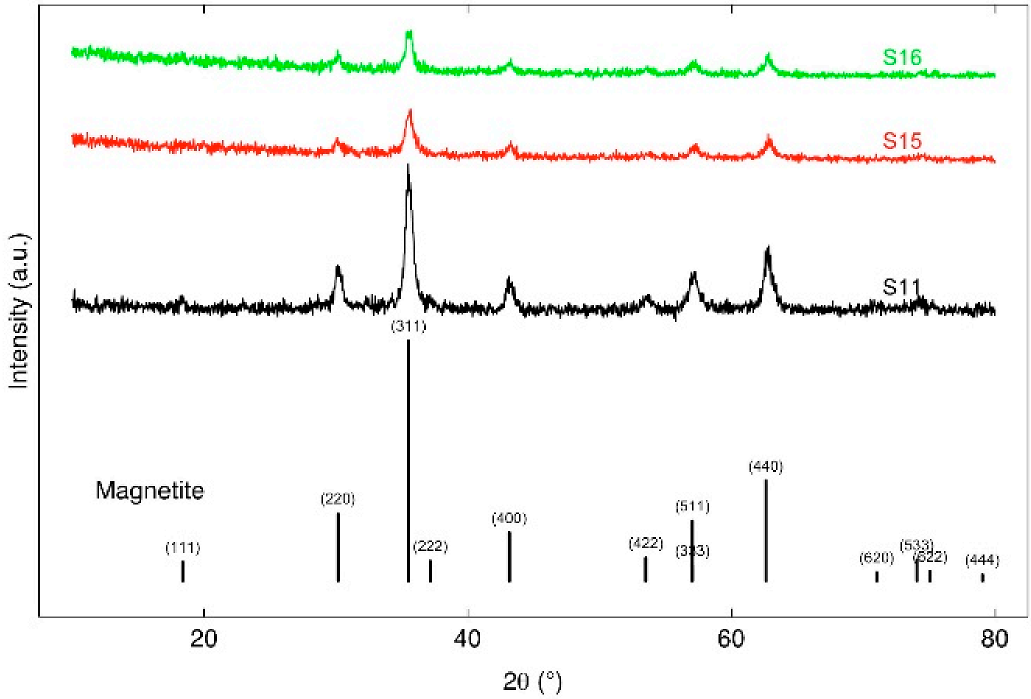

Figure 1. XRD patterns of nanomagnetite-coated biochar powders prepared for 6 h at 200 °C employing: magnetite nanoparticle (S11), 0.18 mm (S15), and 0.38 mm (S16) biochar particles.

The FTIR spectra for samples S11, S15, and S16 are presented in Figure 2a. All three samples show a broad adsorption band around 3193 cm^{-1}, which is indicative of O-H stretching vibrations, likely due to the presence of water or hydroxyl groups adsorption on the surface. Additionally, they display a band at around 1051 cm^{-1}, which is attributed to C-O stretching vibrations. There is also a common peak around 1584 cm^{-1}, corresponding to C=C vibrations. Finally, all three samples show distinct peaks in the 400–600 cm^{-1} range, which are assigned to the Fe-O stretching vibrations characteristic of magnetite [13].

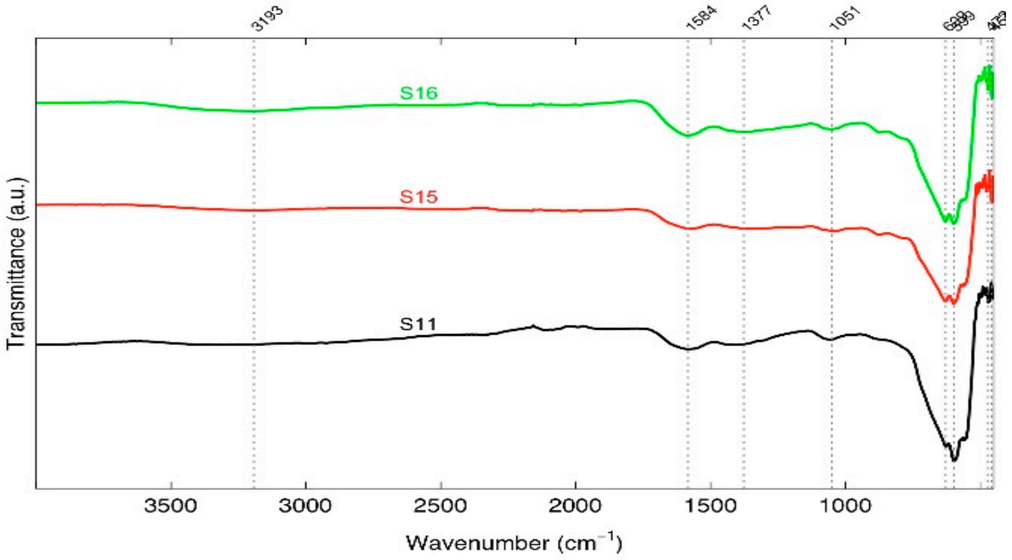

(**a**)

Figure 2. *Cont.*

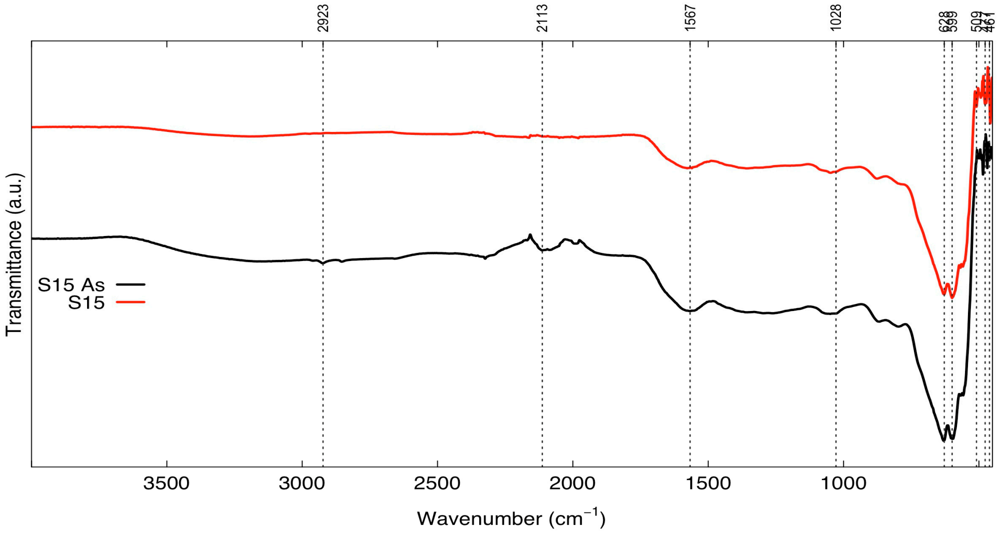

(**b**)

Figure 2. FTIR spectra of (**a**) nanomagnetite-coated biochar (S11, S15, and S16) and (**b**) S15 before and after arsenic adsorption.

The FTIR analysis revealed that magnetite within the composite material participates in arsenic binding, as evidenced by alterations in Fe-O stretching bands below 600 cm^{-1} following adsorption; furthermore, the emergence of a peak around 830 cm^{-1} suggests the formation of Fe-O-As or C-O-As bonds, demonstrating a direct interaction between arsenic species and the adsorbent surface [13].

The scanning electron microscopy (SEM) image (Figure 3) of sample S15, a nanomagnetite-coated biochar synthesized at 200 °C for 6 h, reveals a morphology characterized by homogeneous, spherical particles. These particles exhibit a predominantly spherical shape, indicating a relatively uniform growth process during solvothermal synthesis. The inset image provides a zoomed-in view of these particles, highlighting their smooth and rounded surfaces [5]. Particle size, as observed, is in the nanometer range, with most particles falling within the 95–115 nm range. The SEM image also shows some degree of agglomeration, with individual spherical particles tending to cluster together.

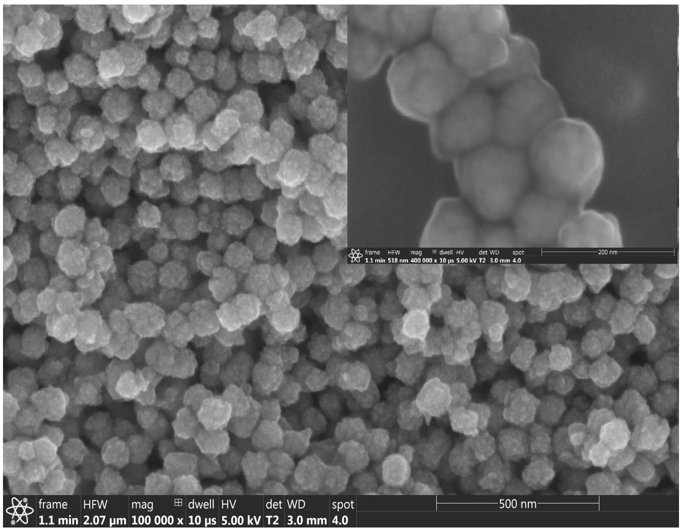

Figure 3. FE-SEM micrograph of nanomagnetite-coated biochar powders prepared for 6 h at 200 °C employing 0.18 mm biochar particles (S15).

3.2. Adsorption Process

Figure 4 displays the arsenic and fluoride removal percentages and adsorption capacities (q_e) for samples S11, S15, and S16. All three samples exhibit exceptionally high arsenic removal percentages, reaching nearly 100%. Among these, S15 demonstrates the highest adsorption capacity (around 6.4 mg/g), followed by S16, and then S11 with the lowest (around 4 mg/g). For fluoride removal, S11 exhibits the lowest performance, while S15 shows the highest, followed by S16.

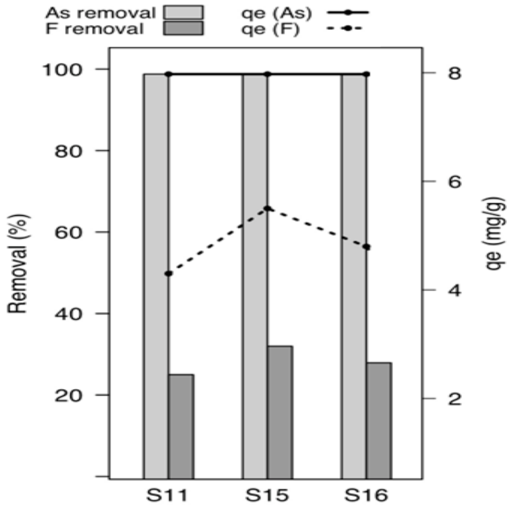

Figure 4. Arsenic and fluoride removal of nanomagnetite-coated biochar powders prepared for 6 h at 200 °C employing: no biochar (S11), 0.18 mm (S15), and 0.38 mm (S16) biochar particles.

4. Discussion

All three samples exhibit XRD patterns consistent with the presence of magnetite. However, the intensities and peak sharpness vary; S11 displays the sharpest and highest intensity peaks, suggesting well-formed and larger magnetite crystals. S15 and S16 show broadened and lower intensity peaks, indicating smaller crystallite sizes and/or lower crystallinity which could be a result of smaller sized magnetite crystals grown on the biochar surface, with S16 being the most broadened. However, the XRD results confirm the formation of magnetite on the S15 and S16 nanomagnetite-coated biochar synthesized at 6 h and 200 °C, indicating a shorter synthesis time than normal for nanomagnetite 10 h [5].

The FTIR analysis (Figure 2) reveals that all three samples contain magnetite, as shown by the presence of the Fe-O bands [13]. The broad O-H band at 3193 cm^{-1} indicates the presence of hydroxyl groups or water adsorption on the surface of all the samples. While the intensity of Fe-O bands is slightly lower in S15 and S16 compared to S11; there is an increase in the band at 1377 and in the band 1051, this is also observed in 1584 and 3193. This confirms that the surface composition of S15 and S16 has more carbon-based groups than S11. The FTIR analysis before and after arsenic adsorption on sample S15 strongly suggests that the removal of arsenic involves a combination of mechanisms, primarily surface complexation with hydroxyl and carbonyl/carboxyl groups present on the nanomagnetite-coated biochar, as well as direct binding to the magnetite surface [14,15]. The biochar component enhances the availability of oxygen-containing functional groups, while the magnetite nanoparticles provide specific binding sites for arsenic species, leading to the high adsorption capacity observed for sample S15.

The SEM image of S15 nanomagnetite-coated biochar shows the successful formation of homogeneous spherical magnetite nanoparticles with a size between 95 and 115 nm. Although the particles show a tendency to agglomerate, they exhibit a consistent morphology that suggests a controlled solvothermal synthesis process.

The enhanced adsorption capacity of S15 over S11 suggests that biochar, by influencing the material's morphology and surface area, significantly contributes to arsenic adsorption, consistent with findings by Shen et al. (2021) [9]. The lower fluoride removal percentages, compared to arsenic, indicate that the material's effectiveness for fluoride removal is limited under the tested conditions. Nevertheless, S15 demonstrated higher efficiency than pure magnetite (S11) and S16, further highlighting the beneficial influence of biochar. Similar observations of higher arsenic removal and lower fluoride removal using biochar were reported by Saikai R. (2017) [16].

The use of biochar in S15 provides a porous support structure with smaller crystallite sizes, as suggested by XRD, this increases surface area and provides more adsorption sites for arsenic compared to the pure magnetite of S11. The presence of biochar enhances the surface groups as suggested by the FTIR results, leading to more surface hydroxyl and carbon-based groups which promote the binding of arsenic ions through various chemical interactions [15]. The small size and spherical shape of the magnetite nanoparticles in S15, as confirmed by SEM, contribute to a high surface-to-volume ratio and provide a large number of active sites for adsorption.

5. Conclusions

This study demonstrates the successful solvothermal synthesis of nanomagnetite-coated biochar from pecan nutshells as an efficient and sustainable arsenic adsorbent. The method produced homogeneously distributed, nanometer-sized magnetite particles on biochar. Sample S15 exhibited exceptional arsenic removal (98.76%) and fluoride (31.97%) significantly higher adsorption capacity than pure magnetite (S11) and larger-sized coated biochar (S16). This is attributed to the synergistic effects of biochar's porous support, enhanced surface functional groups, and optimized nanostructure. While effective for arsenic, the material was less so for fluoride removal. These results highlight the potential of this cost-effective, scalable, and sustainable adsorbent for arsenic remediation in water treatment. Further research could investigate the impact of various solvothermal reaction parameters on the morphology, crystal size, and adsorption capacity of nanomagnetite-coated biochar.

Author Contributions: Conceptualization, S.K.; methodology, S.K. and D.-A.C.-M.; software, A.R.-R.; validation, S.K. and A.R.-R.; formal analysis, S.K. and A.R.-R.; investigation, S.K. and D.-A.C.-M.; resources, L.D.-J. and L.S.-M.; writing—original draft preparation, D.-A.C.-M.; writing—review and editing, S.K. and A.Z.-G.; visualization A.R.-R. All authors have read and agreed to the published version of the manuscript.

Funding: This research received no external funding.

Institutional Review Board Statement: Not applicable.

Informed Consent Statement: Not applicable.

Data Availability Statement: The datasets generated during and/or analyzed during the current study are available from the corresponding author on reasonable request.

Acknowledgments: Khamkure S. gratefully acknowledges the Investigadoras e Investigadores por México SECIHTI program (Project No. CIR/0069/2022). This research was partially supported by the Universidad Autónoma Agraria Antonio Narro (Project No. 38111-425401001-2320). The authors thank Martha E. Rivas-Aguilar and Sergio Rodríguez-Arias for technical characterization, and Socorro García-Guillermo, Jesús Alejandro Espinosa, and María del Socorro Mireles for assistance with chemical analysis.

Conflicts of Interest: The authors declare no conflicts of interest.

References

1. Fatoki, J.O.; Badmus, J.A. Arsenic as an environmental and human health antagonist: A review of its toxicity and disease initiation. *J. Hazard. Mater. Adv.* **2022**, *5*, 100052. [CrossRef]
2. Robledo-Peralta, A.; López-Guzmán, M.; Morales-Amaya, C.G.; Reynoso-Cuevas, L. Arsenic and fluoride in groundwater, prevalence and alternative removal approach. *Processes* **2021**, *9*, 1191. [CrossRef]
3. Cai, G.; Zhu, X.; Li, K.; Qi, X.; Wei, Y.; Wang, H.; Hao, F. Self-enhanced and efficient removal of arsenic from waste acid using magnetite as an in situ iron donator. *Water Res.* **2019**, *157*, 269–280. [CrossRef] [PubMed]
4. De Oliveira, E.C.M.; Caixeta, E.S.; Santos, V.S.V.; Pereira, B.B. Arsenic exposure from groundwater: Environmental contamination, human health effects, and sustainable solutions. *J. Toxicol. Environ. Health Part B* **2021**, *24*, 119–135. [CrossRef] [PubMed]
5. Wang, M.; Ni, Y.; Liu, A. Fe_3O_4@Resorcinol-Formaldehyde Resin/Cu_2O Composite Microstructures: Solution-Phase Construction, Magnetic Performance, and Applications in Antibacterial and Catalytic Fields. *ACS Omega* **2017**, *2*, 1505–1512. [CrossRef] [PubMed]
6. Khamkure, S.; Bustos-Terrones, V.; Benitez-Avila, N.J.; Cabello-Lugo, M.F.; Gamero-Melo, P.; Garrido-Hoyos, S.E.; Esparza-Schulz, J.M. Effect of Fe_3O_4 nanoparticles on magnetic xerogel composites for enhanced removal of fluoride and arsenic from aqueous solution. *Water Sci. Eng.* **2022**, *15*, 305–317. [CrossRef]
7. Khamkure, S.; Díaz-Jiménez, L.; Reyes-Rosas, A.; Gamero-Melo, P.; Zermeño-González, A.; Cortez-Quevedo, E. Magnetic Pecan Nutshell Biochar for Arsenic and Fluoride Removal: Effects of Particle Size and Pyrolysis Temperature. In *Key Engineering Materials*; Trans Tech Publications Ltd.: Aedermannsdorf, Switzerland, 2024; Volume 1003, pp. 101–106. [CrossRef]
8. El-Dib, F.I.; Mohamed, D.E.; El-Shamy, O.A.A.; Mishrif, M.R. Study the adsorption properties of magnetite nanoparticles in the presence of different synthesized surfactants for heavy metal ions removal. *Egypt. J. Pet.* **2020**, *29*, 1–7. [CrossRef]
9. Shen, Z.; Jin, J.; Fu, J.; Yang, M.; Li, F. Anchoring Al- and/or Mg-oxides to magnetic biochars for Co-uptake of arsenate and fluoride from water. *J. Environ. Manag.* **2021**, *293*, 112898. [CrossRef] [PubMed]
10. Vikesland, P.J.; Rebodos, R.L.; Bottero, J.Y.; Rose, J.; Masion, A. Aggregation and sedimentation of magnetite nanoparticle clusters. *Environ. Sci. Nano* **2016**, *3*, 567–577. [CrossRef]
11. Lasheen, M.R.; El-Sherif, I.Y.; Sabry, D.Y.; El-Wakeel, S.T.; El-Shahat, M.F. Adsorption of heavy metals from aqueous solution by magnetite nanoparticles and magnetite-kaolinite nanocomposite: Equilibrium, isotherm and kinetic study. *Desalination Water Treat* **2016**, *57*, 17421–17429. [CrossRef]
12. Liang, S.; Shi, S.; Zhang, H.; Qiu, J.; Yu, W.; Li, M.; Gan, Q.; Yu, W.; Xiao, K.; Liu, B.; et al. One-pot solvothermal synthesis of magnetic biochar from waste biomass: Formation mechanism and efficient adsorption of Cr(VI) in an aqueous solution. *Sci. Total Environ.* **2019**, *695*, 133886. [CrossRef] [PubMed]
13. Zubair, Y.O.; Fuchida, S.; Tokoro, C. Insight into the Mechanism of Arsenic(III/V) Uptake on Mesoporous Zerovalent Iron-Magnetite Nanocomposites: Adsorption and Microscopic Studies. *ACS Appl. Mater. Interfaces* **2020**, *12*, 49755–49767. [CrossRef] [PubMed]
14. He, R.; Peng, Z.; Lyu, H.; Huang, H.; Nan, Q.; Tang, J. Synthesis and characterization of an iron-impregnated biochar for aqueous arsenic removal. *Sci. Total Environ.* **2018**, *612*, 1177–1186. [CrossRef] [PubMed]
15. Bullen, J.C.; Lapinee, C.; Miller, L.A.; Bullough, F.; Berry, A.J.; Najorka, J.; Cibin, G.; Vilar, R.; Weiss, D.J. Spectroscopic (XAS, FTIR) investigations into arsenic adsorption onto TiO_2/Fe_2O_3 composites: Evaluation of the surface complexes, speciation and precipitation predicted by modelling. *Results Surf. Interfaces* **2022**, *9*, 100084. [CrossRef]
16. Saikia, R.; Goswami, R.; Bordoloi, N.; Senapati, K.K.; Pant, K.K.; Kumar, M.; Kataki, R. Removal of arsenic and fluoride from aqueous solution by biomass based activated biochar: Optimization through response surface methodology. *J. Environ. Chem. Eng.* **2017**, *5*, 5528–5539. [CrossRef]